Supporting Information for

Assessing lock-in depth and establishing a Late Holocene paleomagnetic secular variation record from the Mongolian Altai

Marcel Bliedtner, Torsten Haberzettl, Norbert Nowaczyk, Enkhtuya Bazarradnaa, Roland Zech & Paul Strobel

Table S1. ^{14}C-dating results from Khar Nuur modified after Bliedtner et al. (2021). ^{14}C-dating results of the modern water plant (KN_wp) and the surface sediment bulk organic carbon sample (KN_surface) were previously published by Strobel et al. (2021) and calibrated with the bomb peak NH1 calibration dataset (Hua et al., 2013). All other ^{14}C-dating results were previously published by Bliedtner et al., (2021) and calibrated with the IntCal20 calibration curve (Reimer et al., 2020). Please note that the presented bulk organic carbon ^{14}C-ages are not reservoir corrected.

Lab code	Sample label	Depth (cm)	Material	$F^{14}C \pm u$	Conven-tional ages	Calibrated age ranges (cal. BP)	Calibrated median ages (cal. BP)	Calibrated mean ages (cal. BP)	σ
BE-13607.1.1	KN_wp		modern water plant	1.0738±0.0130	-572±98	(-6)-(60) (95.4 %)	-54	-51	11
BE-13608.1.1	KN_surface		surface sediment bulk organic carbon	1.0107±0.0132	-86±105	(-7)-279 (95.4 %)	117	129	85
BE-9765.1.1	KN18_10	10	bulk organic carbon	0.9166±0.0157	700±138	496-921 (95.4 %)	661	671	113
BE-15208.1.1	KN18_10M	10	aquatic macrofossil	0.9204±0.0174	667±152	330-924 (95.4 %)	638	646	126
BE-12032.1.1	KN18_20	20	bulk organic carbon	0.8371±0.0189	1429±181	960-1703 (95.4 %)	1336	1337	189
BE-15221.1.1	KN18_30	30	bulk organic carbon	0.7673±0.0078	2127±82	1898-2334 (95.4 %)	2108	2117	116
BE-15210.1.1	KN18_30M	30	aquatic macrofossil	0.8813±0.0085	1015±78	734-1172 (95.4 %)	916	914	92
BE-9766.1.1	KN18_40	40	bulk organic carbon	0.7615±0.0115	2189±121	1834-2668 (95.4 %)	2178	2180	162
BE-15211.1.1	KN18_40M	40	aquatic macrofossil	0.8250±0.0147	1545±143	1176-1775 (95.4 %)	1453	1460	142
BE-12031.1.1	KN18_52	52	bulk organic carbon	0.7819±0.0088	1976±90	1706-2287 (95.4 %)	1909	1914	120
BE-15212.1.1	KN18_52M	52	aquatic macrofossil	0.7881±0.0211	1913±215	1374-2350 (95.4 %)	1859	1873	259
BE-9767.1.1	KN18_66	66	bulk organic carbon	0.7734±0.0125	2064±130	1730-2339 (95.4 %)	2029	2034	169
BE-15213.1.1	KN18_66M	66	aquatic macrofossil	0.7944±0.0134	1849±135	1416-2113 (95.4 %)	1767	1771	165
BE-12030.1.1	KN18_78	78	bulk organic carbon	0.7227±0.0084	2609±93	2367-2922 (95.4 %)	2706	2676	135
BE-12029.1.1	KN18_90	90	bulk organic carbon	0.6595±0.0077	3343±94	3386-3830 (95.4 %)	3583	3592	115
BE-15215.1.1	KN18_100M	100	aquatic macrofossil	0.7079±0.0108	2775±123	2542-3325 (95.4 %)	2912	2924	151
BE-15220.1.1	KN18_100_Os	100	ostracod shell	0.7023±0.0093	2839±106	2754-3315 (95.4 %)	2976	2987	134
BE-9768.1.1	KN18_110	110	bulk organic carbon	0.6585±0.0118	3356±144	3250-3982 (95.4 %)	3610	3619	177
BE-15216.1.1	KN18_110M	110	aquatic macrofossil	0.6772±0.0065	3131±77	3081-3549 (95.4 %)	3338	3330	93

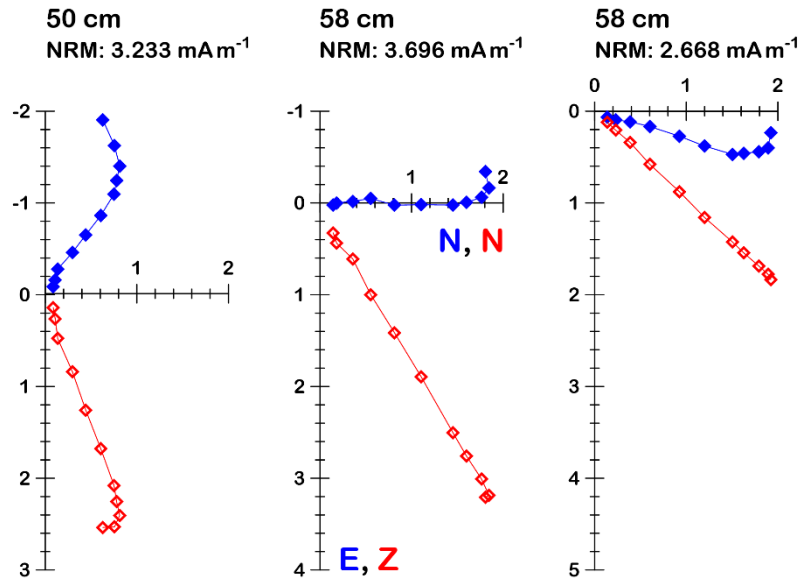| BE-12477.1.1 | KN18_120 | 120 | bulk organic carbon | 0.6356±0.0076 | 3641±97 | 3694-4240 (95.4 %) | 3966 | 3970 | 139 |
BE-15217.1.1	KN18_120M	120	aquatic macrofossil	0.6562±0.0110	3385±134	3350-4062 (95.4 %)	3640	3650	166
BE-12028.1.1	KN18_128	128	bulk organic carbon	0.6192±0.0076	3850±99	3979-4523 (95.4 %)	4260	4257	143
BE-9769.1.1	KN18_141	141	bulk organic carbon	0.6000±0.0113	4104±151	4153-5035 (95.4 %)	4615	4612	210

Figure SI 1. Z-plots from three representative different levels. Closed (blue) symbols represent data in the horizontal plane and open (red) symbols represent data in the vertical plane, with axis orientations as indicated in the middle. Demagnetization steps are: 0, 5, 10, 15, 20, 30, 40 ,50 ,65, 80, 100 mT.
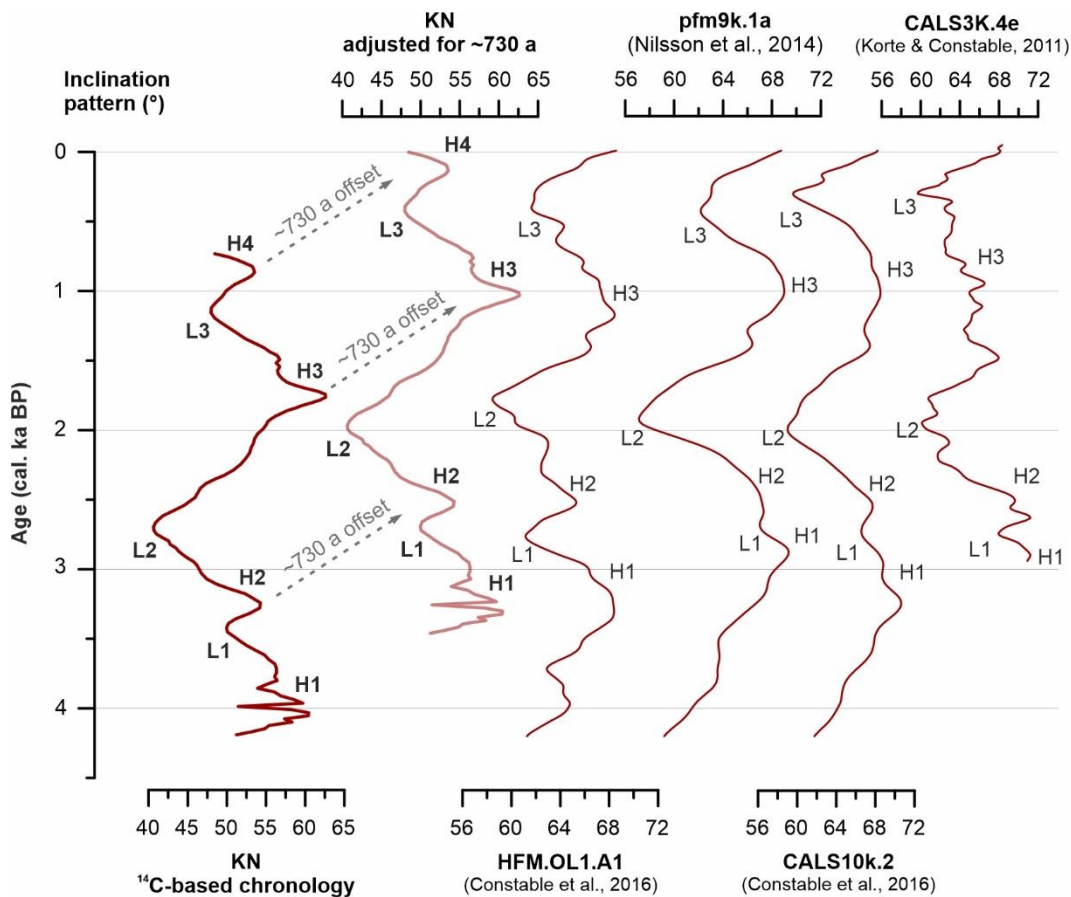

Figure SI 2. Comparison of inclination pattern of the Khar Nuur sediments with the outputs of spherical harmonic geomagnetic field models models (Constable et al., 2016, Korte & Constable, 2011) Nilsson et al., 2014) calculated for the coring position.

References

Bliedtner, M., Struck, J., Strobel, P., Salazar, G., Szidat, S., Bazarradnaa, E., Lloren, R., Dubois, N., Zech, R., 2021. Late Holocene Climate Changes in the Altai Region Based on a First High-Resolution Biomarker Isotope Record From Lake Khar Nuur. Geophys. Res. Lett. 48(20). doi:10.1029/2021GL094299.

Constable, C., Korte, M., Panovska, S., 2016. Persistent high paleosecular variation activity in southern hemisphere for at least 10 000 years. Earth and Planetary Science Letters 453, 78-86, doi:10.1016/j.epsl.2016.08.015.

Hua, Q., Barbetti, M., Rakowski, A.Z., 2013. Atmospheric radiocarbon for the period 1950–2010. Radiocarbon, 55(4), 2059–2072. https://doi.org/10.2458/azu_js_rc.v55i2.16177.

Korte, M., Constable, C., 2011. Improving geomagnetic field reconstructions for 0–3 ka. - Physics of the Earth and Planetary Interiors 188, 3-4, 247-259. doi:10.1016/j.pepi.2011.06.017.

Nilsson, A., Holme, R., Korte, M., Suttie, N., Hill, M., 2014. Reconstructing Holocene geomagnetic field variation: new methods, models and implications. Geophysical Journal International 198, 1, 229-248, doi:10.1093/gji/ggu120.

Reimer, P.J., Austin, W.E.N., Bard, E., Bayliss, A., Blackwell, P.G., Bronk Ramsey, C., et al. 2020. The IntCal20 Northern Hemisphere Radiocarbon Age Calibration Curve (0-55 Cal kBP). Radiocarbon 62, 725–757. doi:10.1017/ RDC.2020.41.

Strobel, P., Struck, J., Zech, R., Bliedtner, M., 2021. The spatial distribution of sedimentary compounds and their environmental implications in surface sediments of Lake Khar Nuur (Mongolian Altai). Earth Surf. Process. Landforms 46(3), 611–625. doi:10.1002/esp.5049.